HHS Public Access

Author manuscript

Exp Physiol. Author manuscript; available in PMC 2016 July 01.

Published in final edited form as:

Exp Physiol. 2015 July 1; 100(7): 805–817. doi:10.1113/EP085104.

Fractalkine neutralization improves cardiac function after myocardial infarction

Xiaosong Gu[1,2], **Jiang Xu**[1], **Xiao-Ping Yang**[1], **Edward Peterson**[3], and **Pamela Harding**[1]

[1]Hypertension and Vascular Research Division, Department of Internal Medicine, Henry Ford Hospital, Detroit, MI 48202, USA

[2]Department of Cardiology, The Second Affiliated Hospital of Soochow University, Suzhou, Jiangsu 215004, China

[3]Department of Public Health Sciences, Henry Ford Hospital, Detroit, MI 48202, USA

Abstract

Concentrations of the chemokine fractalkine (FKN) are increased in patients with chronic heart failure, and our previous studies show that aged mice lacking the prostaglandin E_2 EP4 receptor subtype (EP4-KO) have increased cardiac FKN, with a phenotype of dilated cardiomyopathy. However, how FKN participates in the pathogenesis of heart failure has rarely been studied. We hypothesized that FKN contributes to the pathogenesis of heart failure and that anti-FKN treatment prevents heart failure induced by myocardial infarction (MI) more effectively in EP4-KO mice. Male EP4-KO mice and wild-type littermates underwent sham or MI surgery and were treated with an anti-FKN antibody or control IgG. At 2 weeks post-MI, echocardiography was performed and hearts were excised for determination of infarct size, immunohistochemistry and Western blot of signalling molecules. Given that FKN protein levels in the left ventricle were increased to a similar extent in both strains after MI and that anti-FKN treatment improved survival and cardiac function in both strains, we subsequently used only wild-type mice to examine the mechanisms whereby anti-FKN is cardioprotective. Myocyte cross-sectional area and interstitial collagen fraction were reduced after anti-FKN treatment, as were macrophage migration and gelatinase activity. Activation of ERK1/2 and p38 MAPK were reduced after neutralization of FKN. *In vitro*, FKN increased fibroblast proliferation. In conclusion, increased FKN contributes to heart failure after MI. This effect is not exacerbated in EP4-KO mice, suggesting that there is no link between FKN and lack of EP4. Overall, inhibition of FKN may be important to preserve cardiac function post-MI.

Corresponding author P. Harding: Hypertension and Vascular Research Division, Henry Ford Hospital, E & R Building, Room 7096, 2799 West Grand Boulevard, Detroit, MI 48202, USA. phardin1@hfhs.org.

Competing interests

None declared. The results presented in this paper were presented in abstract form at the Council for High Blood Pressure Research Annual Meeting, San Francisco, September 2014.

Author contributions

Study design: P.H. Myocardial infarction, Western blot, gelatinase activity and immunohistochemistry: X.G. Echocardiography: X.G., J.X. and X.-P.Y. Data analysis: E.P. Initial draft of manuscript: P.H. and X.G. Manuscript editing and final approval: X.G., J.X., X.-P.Y., E.P. and P.H.

Introduction

Fractalkine (FKN), also known as CX3CL1, is the only member of the CX_3C chemokine family, characterized by the presence of three amino acid residues (X_3) localized between two cysteine residues, thus forming a disulfide bond, a CX3C motif, and also a transmembrane domain. The full-length fractalkine protein consists of 397 amino acids encoded by the *CX3CL1* gene mapped on chromosome 16 in humans (Pan *et al.* 1997; Bazan *et al.* 1997) and of 395 amino acids encoded by the neurotactin gene mapped on chromosome 11 in mice (Rossi *et al.* 1998). Fractalkine is a unique dual-function chemokine that exists in two forms; a soluble form, which acts as a chemoattractant, and a membrane-bound form acting as an adhesion molecule (Umehara *et al.* 2004). Fractalkine, its receptor CX3CR1 and monocyte chemoattractant protein 1 have been identified as chemokines and receptors that have an important role in the migration and recruitment of monocytes during the pathogenesis of several inflammatory diseases, including atherosclerosis (Zhou *et al.* 2012). Fractalkine was recently identified as an independent key factor in the pathogenesis of plaque vulnerability and subsequent plaque rupture (Li *et al.* 2012). Fractalkine has also been associated with cardiac injury. Patients with acute myocardial infarction (MI) had significantly elevated levels 3 and 12 h after percutaneous coronary intervention compared with patients who had stable angina pain (Njerve *et al.* 2014). Thus, FKN has a very important role in the pathology of coronary heart disease.

Myocardial infarction is one of the most frequent causes of death. More than 20% of cardiovascular deaths are caused by coronary heart disease (Go *et al.* 2013). Furthermore, even though many patients survive an acute MI, most of them inevitably suffer from heart failure (HF; Fox *et al.* 2001), which is likely to result from left ventricular (LV) remodelling, leading to functional decompensation and then HF (Sutton & Sharpe, 2000). Previous studies have confirmed that ischaemia-induced myocardial fibrosis, inflammation and apoptosis are essential factors in the process of cardiac remodelling after MI (Porter & Turner, 2009). There are few studies that have examined the effects of FKN on models of cardiac injury. Xuan *et al.* (2011) showed that inhibition of FKN reduces cardiac remodelling after transaortic constriction or MI. However, their study did not examine the effects of FKN neutralization on macrophage migration, matrix metalloproteinase activity, myocyte apoptosis or fibroblast proliferation, and a neutralizing antibody was given after the initial wave of inflammation. Also, our study differs from theirs in that we examined the effect of anti-FKN in a cardiac myocyte-selective model of mice lacking the prostaglandin E_2 EP4 receptor subtype (EP4-KO), because our earlier studies had shown that older EP4-KO mice had elevated cardiac concentrations of this chemokine. Thus, the mechanism whereby anti-FKN affects the infarcted heart is still not established.

In a previous study from our laboratory, FKN was increased in left ventricular samples from old male EP4-KO mice that displayed a phenotype of dilated cardiomyopathy with reduced ejection fraction (Harding *et al.* 2010), indicating that prostaglandin E_2 acting on its EP4 receptor protects the heart from ischaemic injury. Thus, in the present study we hypothesized that FKN contributes to heart failure and that treatment with anti-FKN prevents heart failure induced by MI. Furthermore, we hypothesized that FKN neutralization would be more effective in EP4-KO mice.

Methods

Ethical approval

All animal experiments were approved by the Henry Ford Health System Institutional Animal Care and Use Committee in accordance with Federal guidelines.

Generation and genotyping of EP4-KO mice

Generation of cardiac myocyte-specific EP4-KO by a Cre-mediated process has been described previously. Genotyping and breeding details have also been described previously (Harding *et al.* 2010). In our initial experiments, we used both wild-type (WT) and EP4-KO mice. Importantly, these mice are on a mixed genetic background and differ only by the presence or absence of Cre. As our initial experiments in this study showed no difference between strains in their response to anti-FKN, subsequent experiments used only WT mice.

Culture of adult mouse cardiac fibroblasts

Adult mouse cardiac fibroblasts were obtained using a modification of the technique designed to harvest adult mouse cardiac myocytes. Briefly, mice were anaesthetized by inhalation of isoflurane (3% isoflurane with 1 l min^{-1} oxygen), their hearts were removed and a cannula inserted into the aorta for retrograde perfusion. Mouse hearts were then digested as described previously by us (Harding *et al.* 2010), and the supernatant obtained after digestion was removed. This supernatant was centrifuged at 100*g* for 1 min (4°C), and the resulting supernatant, which contains the fibroblasts, was centrifuged at 145*g* and the pellet resuspended in 5 ml of Dulbecco's modified Eagle's medium containing 10% fetal calf serum. Cells were plated on a 60 mm dish and after 2–3 h, the medium was gently removed and fresh medium added. Cells were allowed to grow and typically passaged at a ratio of 1:3. All experiments on cardiac fibroblast proliferation were performed using hearts from 10- to 12-week-old male C57BL/6 mice, and cells were used at passage 3.

Fractalkine enzyme-linked immunosorbent assay (ELISA)

Fractalkine was measured in left ventricular homogenates using a quantitative sandwich enzyme immunoassay (Mouse CX3CL1/Fractalkine Quantikine ELISA, catalogue no. MCX310; R&D Systems Minneapolis, MN, USA). Left ventricular homogenates were centrifuged at 10,000*g* for 10 min at 4°C. After centrifugation, 100 μl of supernatant was subjected to ELISA according to the manufacturer's instructions. Samples were measured in duplicate and fractalkine concentrations normalized to total tissue protein, respectively, which was determined in lysates according to the method of Lowry.

Myocardial infarction model and treatment with fractalkine neutralizing antibody (anti-FKN)

Male mice 10–12 weeks old were anaesthetized with pentobarbital (45 mg kg^{-1}) (Akorn, Inc., Lake Forest, IL. USA), intubated, and ventilated with a small rodent ventilator (Harvard Apparatus, Holliston, MA, USA) at a rate of 90 cycles min^{-1} with a tidal volume of 0.5 ml and a positive end-expiratory pressure of 2 cmH_2O. A left side thoracotomy was performed, and the pericardium was incised. Myocardial infarction was then induced through permanent ligation of the left anterior descending coronary artery with an 8–0 silk

suture proximal to its bifurcation from the main stem. Sham surgery was performed as described above except that the suture was not tied around the artery. The chest incision was subsequently closed with a 4–0 silk suture. Mice were then allowed to recover in a temperature-controlled environment. After surgery, mice were given a dose of buprenorphine (0.05 mg kg^{-1} $_{S.C.}$) every 12 h for 2 days.

We studied the following groups of mice for each strain (the numbers for each group are given in parentheses): WT sham + IgG (8), WT sham + anti-FKN (6), WT MI + IgG (26), WT MI + anti-FKN (25), EP4-KO sham + IgG (7), EP4-KO sham + anti-FKN (5), EP4-KO MI + IgG (29) and EP4-KO MI + anti-FKN (28), for a total of eight different groups. Treatment was started on the day of surgery and continued for 2 weeks. We administered 40 μg kg^{-1} day^{-1} $_{I.P.}$ of a function-blocking anti-FKN antibody that was raised against the chemotactic domain of FKN (purified rabbit anti-mouse fractalkine, TP233; Torrey Pines Biolabs, Houston, TX, USA) or rabbit IgG (Protein Mods, Madison, WI, USA) as described by Xuan *et al.* (2011) and Robinson *et al.* (2000).

Survival

Survival analysis was performed on all mice. During the study period, the cages were inspected daily for dead animals. All dead mice were examined for the presence of MI as well as cardiac rupture.

Echocardiography

Two weeks after MI, cardiac function was measured with a Doppler echocardiographic system equipped with a 15 MHz linear array transducer (Acuson c256, Mountain View, CA, USA). All studies were performed on conscious mice, which is a standard procedure in our laboratory, and as we have previously described (Yang *et al.* 1999; Harding *et al.* 2010, 2011). The following parameters were obtained: (i) LV chamber dimensions and wall thickness, where LVDd is diastolic LV dimension, LVDs is systolic LV dimension and PWTd is diastolic posterior wall thickness; and (i) ejection fraction (LVEF), which is equivalent to [(LVAd – LVAs)/LVAd] × 100, where LVAd is LV diastolic area and LVAs is LV systolic area.

Histological assessment of interstitial collagen fraction (ICF), myocyte cross-sectional area (MCSA), infarct size (IS) of the infarct area

At the end of the experimental period, mice were anaesthetized with sodium pentobarbital (100 mg kg^{-1} $_{I.P.}$) and the heart was injected with 15% potassium chloride, leading to its arrest in diastole. The heart was removed, washed in ice-cold PBS, and the atria and right ventricle were dissected. Mouse left ventricles were harvested and sectioned transversely into four slices from apex to base. Three sections (sections A, B and C) were frozen in isopentane and stored at −80°C for determination of ICF, MCSA and IS, as previously described (Qian *et al.* 2008). Measurements were made using MicroSuite Biological Imaging Software (Melville, NY, USA).

Immunohistochemical staining of fractalkine and macrophages

Frozen sections of left ventricle were used to detect both FKN and macrophage infiltration. Tissue sections (5 μm thick) were allowed to reach room temperature and were then fixed in ice-cold acetone for 10 min. Sections were incubated with 3% hydrogen peroxide to quench endogenous peroxidase, rinsed, and then incubated with 1% bovine serum albumin for 10 min before incubation with primary antibodies against FKN at 1:200 dilution (Cx3Cl1, catalogue no. ab25088; Abcam Cambridge, MA. USA) or the macrophage marker CD68 at 1:200 dilution (CD68, catalogue no. MCA1957; AbD Serotec, Raleigh, NC. USA) at 4°C overnight. Sections were rinsed and then incubated for 40 min with a biotinylated rabbit anti-rat antibody, rinsed, and then incubated with avidin–biotin complex reagent for 40 min. Bound antibodies were visualized following incubation with AEC (3-amino-9-ethylcarbazole) single solution (Invitrogen, Carsbad, CA, USA) for 3–5 min. Sections of experimental tissue were incubated with isotype-matched normal antibody as a negative control. Sections were counterstained with Mayer's Haematoxylin and dehydrated for microscopic examination. Images were digitally quantified using the ImageJ system (version 1.42; National Institutes of Health, Bethesda, MD, USA) with CD68 positivity assessed in the remote zone and expressed as the number of macrophages per square millimetre.

Effect of fractalkine on fibroblast proliferation

The effect of FKN on proliferation of adult mouse fibroblasts (AVFs) was determined using the TACS MTT cell proliferation kit (Trevigen Inc., Gaithersburg, MD, USA). Briefly, AVFs were cultured until passage 2, and at ~90% confluence were seeded onto a 96-well plate at a density of 20,000 cells per well. They were allowed to attach overnight and were then serum starved for 24 h. Cells were treated with FKN (0–200 ng ml^{-1}) for 24 h in fresh media without serum and were then processed according to the manufacturer's instructions. Absorbance was measured at 550 nm using a plate reader, and the average reading of wells without cells (blanks) was subtracted from each measurement. All samples were assayed in triplicate.

TUNEL staining for apoptosis

Serial 5-μm-thick sections of left ventricles were cut onto slides. After storage at −80°C, frozen sections were allowed to come to room temperature for 5 min, and then apoptosis-related DNA fragmentation was determined by the terminal deoxynucleotidyl transferase dUTP nick end labelling (TUNEL) assay using a TUNEL Apoptosis Detection Kit (Millipore, Temecula, CA, USA) following the manufacturer's instructions. Specimens were examined and photographed with a Nikon eclipse E600 light microscope. Images were captured with the NIS-Elements BR imaging software. On TUNEL-stained sections, apoptotic cells in the border zone were quantified by counting the number of cells in randomly selected fields of a total of five sections. The apoptotic index was expressed as the number of apoptotic cells per field.

Protein extraction and Western blot analysis

Protein was isolated from samples of left ventricle after homogenization in a lysis buffer containing 150 mM NaCl, 50 mM Tris–Cl (pH 7.5), 0.5% deoxycholate, 0.1% SDS and 1%

nonidet P-40 with phosphatase and protease inhibitor tablets (PhosSTOP and Complete Mini, EDTA-free protease inhibitor cocktail tablets; Roche Diagnostics, Indianapolis, IN. USA). After homogenization, samples were centrifuged at 3000*g* for 10 min (4°C), and the supernatants were removed for Western blot analysis. The protein concentration was determined with the Coomassie protein assay kit using bovine serum albumin as the standard. Aliquots of samples (50 μg protein) were subjected to SDS-PAGE and electrotransferred to a polyvinyl difluoride membrane at 36 V overnight at 4°C. The membrane was incubated in 5% non-fat milk in PBS containing 0.1% Tween 20 (PBS-T) for 1 h at room temperature and then overnight at 4°C in the same buffer containing primary antibodies to phospho-p38 mitogen-activated protein kinase (p-p38 MAPK, catalogue no. 4511S; p38 MAPK, catalogue no. 9212S; Cell Signaling, Danvers, MA. USA) or phospho-extracellular regulated signal kinase 1/2 (p-ERK1/2, catalogue no. 9101 L; ERK1/2, catalogue no. 9102; Cell Signaling). The membrane was washed with PBS-T and incubated with horseradish peroxidase-conjugated secondary antibody at room temperature for 1 h. After being washed, the membrane was developed with SuperSignal West Pico Chemiluminescent reagent (Thermoscientific, Rockford, IL. USA) at room temperature. The signal was detected through an exposure to Fuji RX film and analysed by scanning densitometry. The target protein was normalized to the loading control and expressed as the fold increase *versus* control.

In situ zymography

In situ zymography was performed on frozen sections as previously described (Tsujita *et al.* 2007). Fluorescein-conjugated, dye-quenched gelatin from pig skin (DQ™-gelatin) was obtained from Molecular Probes (Invitrogen, Basel, Switzerland). A 1 mg ml^{-1} stock solution of DQ-gelatin was prepared in gelatinase reaction buffer (150 mM NaCl, 5 mM $CaCl_2$, 0.2 mM NaN_3 and 50 mM Tris–HCl, pH 7.6) and stored at 4°C. The working solution for *in situ* zymography was made by directly diluting DQ-gelatin stock solution in reaction buffer to a final concentration of 20 μg ml^{-1}. Unfixed cryosections were thawed, rounded with a wax pen, overlaid with 25 μl DQ-gelatin working solution and incubated at 37°C in an humidified dark chamber for 5 h, and pictures were immediately taken under the microscope. Control sections were incubated in the presence of 20 mM EDTA, which inhibits gelatinase activity. Digital images showing the infarction borders were taken under the ×20 objective, and a threshold was set using ImageJ software that encompassed only the bright green fluorescence indicative of gelatinase activity. The percentage area of gelatinase activity was calculated for each animal per field and the mean calculated for each group.

Statistical analyses

Results are shown as means ± SEM. Comparisons among groups were analysed using one-way ANOVA followed by Hochberg's *post hoc* test. Comparisons between two independent groups were analysed using Student's unpaired *t* test when variances were equal, and a Satterwaite correction was used when variances were different. A log rank test was used to compare survival distributions. Values of $P < 0.05$ were considered to be statistically significant.

Results

Fractalkine expression in mouse heart

Fractalkine protein levels were increased in the hearts of mice failing because of induced MI. The results of immunohistochemistry clearly showed increased expression of FKN protein in infarcted hearts (Fig. 1). Suprisingly, quantitative analysis using ELISA on samples of homogenized left ventricle showed that FKN protein was not different between sham WT and sham EP4-KO. Furthermore, FKN protein increased in both strains after MI, with no statistical difference between strains (bar graph in Fig. 1).

Anti-fractalkine treatment improves survival after MI

After MI, we observed ~60% mortality, which did not differ between strains (Fig. 2), with the majority of mice dying within the first 7 days, due to cardiac rupture. Treatment with anti-FKN improved the survival rate in both strains. In WT mice treated with anti-FKN, 16 mice from a total of 25 mice survived (64% survival rate), whereas only 11 mice from a total of 26 mice given control IgG survived (42% survival rate, $P < 0.05$; Fig. 2 left panel). Similar effects were noted in EP4-KO mice, where 19 of 28 mice treated with anti-FKN survived (68% survival), whereas only 12 of 29 given IgG survived (41% survival, $P < 0.05$; Fig. 2 right panel).

Anti-fractalkine treatment improves cardiac function after MI

All echocardiography data for WT mice are presented in Table 1, and representative echocardiography data are shown in Fig. 3*A*, with quantitative data for ejection fraction (LVEF) and left ventricular dimension at systole (LVDs) depicted in Fig. 3*B* and *C*, respectively. As expected, 2 weeks post-MI there were significant decreases in LVEF accompanied by increases in LVDs for both strains. Anti-fractalkine treatment increased LVEF in both EP4-KO and WT mice after MI (Fig. 3*B*), suggesting improved cardiac function after FKN neutralization. Likewise, the increase in left ventricular dimension after MI was significantly reduced by anti-FKN treatment in WT mice (from 4.3 ± 0.44 to 2.48± 0.44 mm for systole and from 5.03 ± 0.31 to 3.74 ± 0.35 mm for diastole, $P < 0.01$).

Thus, contrary to our original hypothesis, anti-FKN treatment was equally effective in both strains; therefore, our subsequent studies examined the mechanisms responsible for this protective effect in WT mice only.

Anti-fractalkine treatment reduces infarct size and prevents cardiac hypertrophy and remodelling after MI

Trichrome staining was used to detect the size of the infarcted area 2 weeks post-MI. Infarct size was significantly reduced after treatment with anti-FKN (Fig. 4).

As expected, both MCSA and ICF were increased following MI, and Fig. 5*B* demonstrates that both parameters were reduced by anti-FKN treatment.

Anti-fractalkine treatment reduces macrophage infiltration

To investigate the underlying mechanism(s) contributing to the protection afforded by anti-FKN treatment, we analysed macrophage infiltration in LV sections taken 14 days after MI. As expected, immunohistochemistry demonstrated a significantly increased number of macrophages (CD68 positive) in mice subject to MI compared with sham-operated mice. Figure 6 shows that anti-FKN treatment decreased macrophage infiltration in the remote zone post-MI, suggesting that anti-FKN treatment reduces macrophage activation and inflammation after MI.

Anti-fractalkine treatment inhibits apoptosis post-MI

At 14 days after MI, apoptosis levels in the myocardium were determined by TUNEL staining. As shown in Fig. 7, the apoptotic index (number of TUNEL-positive cells per slide) in the MI group was significantly higher than in the sham-operated group, and anti-FKN treatment reduced the number of apoptotic cells post-MI.

Anti-fractalkine treatment reduces gelatinase activity

Figure 8 shows representative *in situ* gelatin zymography of the LV from sham + IgG, MI + IgG and MI + anti-FKN mice. There was minimal matrix metalloproteinase activity in the sham group. Fourteen days after MI, we observed markedly enhanced gelatinase in the LV with significant attenuation of matrix metalloproteinase activity following anti-FKN treatment. The gelatinolytic area in sham-operated mice was 1.32% and was increased to 43.4% in mice subjected to MI. Treatment with the FKN neutralizing antibody reduced the gelatinolytic area to 19.3% ($P < 0.05$ compared with the MI group).

Effect of FKN on proliferation of cultured mouse ventricular fibroblasts

Given that treatment with anti-FKN reduced interstitial collagen fraction, we determined the effect of FKN on proliferation of mouse cardiac fibroblasts *in vitro*. As shown in Fig. 9, treatment with FKN for 24 h significantly increased fibroblast proliferation at concentrations ≥50 ng ml^{-1}. Although the lower concentrations of 5 and 10 ng ml^{-1} also increased proliferation, these changes did not achieve statistical significance ($P = 0.09$ and $P = 0.06$, respectively).

Anti-fractalkine treatment reduces phosphorylation of p38 MAPK and ERK1/2 MAPK after MI

Consistent with previously reported data, Fig. 10 shows that both phospho-p38 and phospho-ERK1/2 are increased in the left ventricle following MI. Treatment with anti-FKN reduced the increases noted after MI, whereas anti-FKN had no effect on these MAPKs in sham-operated animals.

Discussion

This study demonstrates that anti-FKN therapy significantly retards remodelling and HF in both WT and EP4-KO mice after myocardial infarction. The key findings in this study are as follows: (i) anti-FKN therapy improved survival after permanent occlusion of the left

anterior descending coronary artery in comparison to treatment with control IgG; (ii) anti-FKN therapy led to a significant reduction in infarct size after MI and remarkable improvements in cardiac remodelling and function during HF; (iii) anti-FKN therapy attenuated macrophage infiltration into heart tissue during MI and inhibited myocyte apoptosis, and *in vitro* tests also showed that FKN increased the proliferation of adult mouse cardiac fibroblasts; and (iv) anti-FKN-mediated cardioprotection was associated with a decrease in gelatinase activity and phosphorylation of p38 MAPK and ERK1/2. These data provide additional insights into the pleiotropic effects of FKN in cardiovascular disease and its therapeutic role in ischaemia-induced HF.

Our previous study reported that FKN expression and production were increased in the hearts of aged (28- to 32-week-old) male EP4-KO mice (Taube *et al.* 2013), whereas our present study used younger mice subjected to MI and showed that FKN expression and production was increased in both WT and EP4-KO mice. Cardiac function data showed that the effects of FKN neutralization were similar in both strains, so we concluded that the presence or absence of the EP4 receptor does not affect responses to anti-FKN and we performed subsequent experiments using only the one strain. These results are consistent with our data showing that neither prostaglandin E_2 nor an EP4 agonist regulates FKN from cardiac myocytes (Taube *et al.* 2013).

In clinical investigations, expression of CX3CL1 (FKN) in endomyocardial biopsy was significantly increased in enterovirus-positive and virus-negative patients with myocarditis (Escher *et al.* 2011). Circulating levels of CX3CL1 were also increased in patients with chronic HF in accordance with disease severity [1.6-fold in New York Heart Association (NYHA) grade II, 2.2-fold in NYHA grade III and 2.9-fold in NYHA grade IV], with CX3CL1 protein production increased in both cardiomyocytes and fibrous tissue. However, in addition to FKN being a marker for heart failure, *in vitro* experiments showed that the addition of FKN to neonatal cardiomyocytes could induce the expression of markers of cardiac hypertrophy and protein phosphatases. Taken together with recent data from our laboratory showing that FKN can reduce the magnitude and speed of contraction in adult mouse myocytes, the data suggest that FKN may have a pathophysiological role in heart failure and that its inhibition or neutralization may be an effective therapeutic strategy (Husberg *et al.* 2008).

In our study, we found that the majority of mice died within 1 week following MI surgery, primarily due to cardiac rupture, and anti-FKN treatment remarkably reduced mortality. To elucidate the mechanism, we investigated the change of inflammation and apoptosis after MI. Inflammation is a crucial factor in the post-MI healing process. An excessive inflammatory response in the infarcted myocardium is related to adverse cardiac events, including cardiac rupture, and anti-inflammation therapy can protect from cardiac rupture (Anzai, 2013). Another important factor determining survival is apoptosis. Myocardial remodelling following MI is emerging as a key cause of chronic heart failure. Following MI, both the infarcted region and the remote non-infarcted zone undergo cardiac remodelling as a part of the wound-healing response. The LV healing response can be divided into two overlapping phases. The first step is ischaemia-induced myocyte necrosis, as cardiomyocyte death triggers the rapid activation of the complement system. Next, the viable

cardiomyocytes undergo compensatory hypertrophy, which helps to maintain cardiac output (Stefanon *et al.* 2013; Shinde & Frangogiannis, 2014). At the same time, fibroblasts proliferate and release fibrosis-promoting cytokines that contribute positively to scar formation, with the net result being increased extracellular matrix synthesis and deposition (Shinde & Frangogiannis, 2014). Myocyte cross-sectional area and ICF, indices of cardiac hypertrophy and fibrosis, were both examined in the present study. Anti-FKN treatment reduced both the increased MCSA and ICF after MI, accompanied by an improvement in cardiac function. Subsequent *in vitro* experiments showed that FKN increased adult mouse cardiac fibroblast proliferation; a novel finding that supports the *in vivo* data showing that anti-FKN reduces the deposition of interstitial collagen. As expected, apoptosis was increased after MI, and this effect was reduced by anti-FKN treatment. Moreover, we also observed decreased macrophage migration and gelatinase activity following anti-FKN treatment, which would be expected to limit cardiac remodelling.

In the present study, we began to elucidate how neutralization of FKN exerts protective effects. Many signalling pathways have previously been implicated in the pathology of MI. Both ERK1/2 and p38 MAPK have widely been reported in the remodelling of heart disease, (Liu *et al.* 2005; Lei *et al.* 2013; Pramod & Shivakumar, 2014), with Liu *et al.* (2005) reporting that inhibition of p38 MAPK reduces MCSA and ICF. It has been suggested that activation of ERK1/2 promotes cardiac inflammation, hypertrophy and fibrosis (Kehat & Molkentin, 2010). In cultured cardiac fibroblasts, FKN-induced phosphorylation of ERK1/2 participates in angiotensin II-mediated inflammation, myocardial injury and dysfunction (Song *et al.* 2013). In human microvascular endothelial cells and human umbilical vein endothelial cells, FKN induces significant alterations in cytoskeletal structure and specifically activates MAPKs (Volin *et al.* 2010), suggesting that FKN can induce pathological changes in the heart by these pathways. In support of these previous studies, the present study shows that anti-FKN treatment reduces the enhanced ERK1/2 phosphorylation and p38 MAPK phosphorylation observed after MI.

In conclusion, the present study has demonstrated that anti-FKN treatment has a cardioprotective effect in both EP4-KO and WT mice subject to MI. In contrast to our original hypothesis, EP4-KO mice did not have an exaggerated response to FKN neutralization, and FKN levels after MI were similar in both strains. Our end-points focused on functional and pathophysiological changes and histological remodelling of the heart, with a preliminary examination of the molecular and cellular mechanisms and signalling pathways that lead to the cardioprotective effect of FKN neutralization in this particular model. Whether a similar approach would be protective in other models of cardiac injury or in the clinical setting remains to be elucidated.

Acknowledgements

The authors would like to thank David Taube and Gulser Gurocak for excellent technical assistance. Thanks also to Edward Shesely for the genotyping and maintenance of the EP4-KO mouse colony.

Funding

These studies were funded by a National Institutes of Health grant [5P01HL028982] (sub-project 2) to P.H.

References

Anzai T. Post-infarction inflammation and left ventricular remodeling: a double-edged sword. Circ J. 2013; 77:580–587. [PubMed: 23358460]

Bazan JF, Bacon KB, Hardiman G, Wang W, Soo K, Rossi D, Greaves DR, Zlotnik A, Schall TJ. A new class of membrane-bound chemokine with a CX3C motif. Nature. 1997; 385:640–644. [PubMed: 9024663]

Escher F, Vetter R, Küuhl U, Westermann D, Schultheiss HP, Tschöpe C. Fractalkine in human inflammatory cardiomyopathy. Heart. 2011; 97:733–739. [PubMed: 21357373]

Fox KF, Cowie MR, Wood DA, Coats AJ, Gibbs JS, Underwood SR, Turner RM, Poole-Wilson PA, Davies SW, Sutton GC. Coronary artery disease as the cause of incident heart failure in the population. Eur Heart J. 2001; 22:228–236. [PubMed: 11161934]

Go AS, Mozaffarian D, Roger VL, Benjamin EJ, Berry JD, Borden WB, Bravata DM, Dai S, Ford ES, Fox CS, Franco S, Fullerton HJ, Gillespie C, Hailpern SM, Heit JA, Howard VJ, Huffman MD, Kissela BM, Kittner SJ, Lackland DT, Lichtman JH, Lisabeth LD, Magid D, Marcus GM, Marelli A, Matchar DB, McGuire DK, Mohler ER, Moy CS, Mussolino ME, Nichol G, Paynter NP, Schreiner PJ, Sorlie PD, Stein J, Turan TN, Virani SS, Wong ND, Woo D, Turner MB. Executive summary: heart disease and stroke statistics–2013 update: a report from the American Heart Association. Circulation. 2013; 127:143–152. [PubMed: 23283859]

Harding P, Yang XP, He Q, LaPointe MC. Lack of microsomal prostaglandin E synthase-1 reduces cardiac function following angiotensin II infusion. Am J Physiol Heart Circ Physiol. 2011; 300:H1053–H1061. [PubMed: 21193590]

Harding P, Yang XP, Yang J, Shesely E, He Q, LaPointe MC. Gene expression profiling of dilated cardiomyopathy in older male EP4 knockout mice. Am J Physiol Heart Circ Physiol. 2010; 298:H623–H632. [PubMed: 20008274]

Husberg C, Nygård S, Finsen AV, Damås JK, Frigessi A, Oie E, Waehre A, Gullestad L, Aukrust P, Yndestad A, Christensen G. Cytokine expression profiling of the myocardium reveals a role for CX3CL1 (fractalkine) in heart failure. J Mol Cell Cardiol. 2008; 45:261–269. [PubMed: 18585734]

Kehat I, Molkentin JD. Extracellular signal-regulated kinase 1/2 (ERK1/2) signaling in cardiac hypertrophy. Ann N Y Acad Sci. 2010; 1188:96–102. [PubMed: 20201891]

Lei J, Xue S, Wu W, Zhou S, Zhang Y, Yuan G, Wang J. Sdc1 overexpression inhibits the p38 MAPK pathway and lessens fibrotic ventricular remodeling in MI rats. Inflammation. 2013; 36:603–615. [PubMed: 23264165]

Li J, Guo Y, Luan X, Qi T, Li D, Chen Y, Ji X, Zhang Y, Chen W. Independent roles of monocyte chemoattractant protein-1, regulated on activation, normal T-cell expressed and secreted and fractalkine in the vulnerability of coronary atherosclerotic plaques. Circ J. 2012; 76:2167–2173. [PubMed: 22664781]

Liu YH, Wang D, Rhaleb NE, Yang XP, Xu J, Sankey SS, Rudolph AE, Carretero OA. Inhibition of p38 mitogen-activated protein kinase protects the heart against cardiac remodeling in mice with heart failure resulting from myocardial infarction. J Card Fail. 2005; 11:74–81. [PubMed: 15704068]

Njerve IU, Solheim S, Lunde K, Hoffmann P, Arnesen H, Seljeflot I. Fractalkine levels are elevated early after PCI-treated ST-elevation myocardial infarction; no influence of autologous bone marrow derived stem cell injection. Cytokine. 2014; 69:131–135. [PubMed: 24930044]

Pan Y, Lloyd C, Zhou H, Dolich S, Deeds J, Gonzalo JA, Vath J, Gosselin M, Ma J, Dussault B, Woolf E, Alperin G, Culpepper J, Gutierrez-Ramos JC, Gearing D. Neurotactin, a membrane-anchored chemokine upregulated in brain inflammation. Nature. 1997; 387:611–617. [PubMed: 9177350]

Porter KE, Turner NA. Cardiac fibroblasts: at the heart of myocardial remodeling. Pharmacol Ther. 2009; 123:255–278. [PubMed: 19460403]

Pramod S, Shivakumar K. Mechanisms in cardiac fibroblast growth: an obligate role for Skp2 and FOXO3a in ERK1/2 MAPK-dependent regulation of p27kip1. Am J Physiol Heart Circ Physiol. 2014; 306:H844–H855. [PubMed: 24441545]

Qian JY, Harding P, Liu Y, Shesely E, Yang XP, LaPointe MC. Reduced cardiac remodeling and function in cardiac-specific EP4 receptor knockout mice with myocardial infarction. Hypertension. 2008; 51:560–566. [PubMed: 18180401]

Robinson LA, Nataraj C, Thomas DW, Howell DN, Griffiths R, Bautch V, Patel DD, Feng L, Coffman TM. A role for fractalkine and its receptor (CX3CR1) in cardiac allograft rejection. J Immunol. 2000; 165:6067–6072. [PubMed: 11086038]

Rossi DL, Hardiman G, Copeland NG, Gilbert DJ, Jenkins N, Zlotnik A, Bazan JF. Cloning and characterization of a new type of mouse chemokine. Genomics. 1998; 47:163–170. [PubMed: 9479488]

Shinde AV, Frangogiannis NG. Fibroblasts in myocardial infarction: a role in inflammation and repair. J Mol Cell Cardiol. 2014; 70:74–82. [PubMed: 24321195]

Song B, Zhang ZZ, Zhong JC, Yu XY, Oudit GY, Jin HY, Lu L, Xu YL, Kassiri Z, Shen WF, Gao PJ, Zhu DL. Loss of angiotensin-converting enzyme 2 exacerbates myocardial injury via activation of the CTGF-fractalkine signaling pathway. Circ J. 2013; 77:2997–3006. [PubMed: 24161906]

Stefanon I, Valero-Muñoz M, Fernandes AA, Ribeiro RF Jr, Rodríguez C, Miana M, Martínez-González J, Spalenza JS, Lahera V, Vassallo PF, Cachofeiro V. Left and right ventricle late remodeling following myocardial infarction in rats. PLoS ONE. 2013; 8:e64986. [PubMed: 23741440]

Sutton MG, Sharpe N. Left ventricular remodeling after myocardial infarction: pathophysiology and therapy. Circulation. 2000; 101:2981–2988. [PubMed: 10869273]

Taube D, Xu J, Yang XP, Undrovinas A, Peterson E, Harding P. Fractalkine depresses cardiomyocyte contractility. PLoS ONE. 2013; 8:e69832. [PubMed: 23936109]

Tsujita K, Kaikita K, Hayasaki T, Honda T, Kobayashi H, Sakashita N, Suzuki H, Kodama T, Ogawa H, Takeya M. Targeted deletion of class A macrophage scavenger receptor increases the risk of cardiac rupture after experimental myocardial infarction. Circulation. 2007; 115:1904–1911. [PubMed: 17389263]

Umehara H, Bloom ET, Okazaki T, Nagano Y, Yoshie O, Imai T. Fractalkine in vascular biology: from basic research to clinical disease. Arterioscler Thromb Vasc Biol. 2004; 24:34–40. [PubMed: 12969992]

Volin MV, Huynh N, Klosowska K, Reyes RD, Woods JM. Fractalkine-induced endothelial cell migration requires MAP kinase signaling. Pathobiology. 2010; 77:7–16. [PubMed: 20185962]

Xuan W, Liao Y, Chen B, Huang Q, Xu D, Liu Y, Bin J, Kitakaze M. Detrimental effect of fractalkine on myocardial ischaemia and heart failure. Cardiovasc Res. 2011; 92:385–393. [PubMed: 21840883]

Yang XP, Liu YH, Rhaleb NE, Kurihara N, Kim HE, Carretero OA. Echocardiographic assessment of cardiac function in conscious and anesthetized mice. Am J Physiol Heart Circ Physiol. 1999; 277:H1967–H1974.

Zhou JJ, Wang YM, Lee VW, Phoon RK, Zhang GY, Wang Y, Tan TK, Hu M, Wang LD, Saito M, Sawyer A, Harris DC, Alexander SI, Durkan AM. DEC205-DC targeted DNA vaccines to CX3CR1 and CCL2 are potent and limit macrophage migration. Int J Clin Exp Med. 2012; 5:24–33. [PubMed: 22328945]

New Findings

- What is the central question of this study?

  What is the cardioprotective role of fractalkine neutralization in heart failure and what are the mechanisms responsible?

- What is the main finding and its importance?

  The concentration of fractalkine is increased in the left ventricle of mice with myocardial infarction, similar to the increases in plasma from heart failure patients. The present study shows a clear beneficial effect of neutralizing fractalkine in a model of myocardial infarction, which results in increased survival. Such an approach may be worthwhile in human patients.

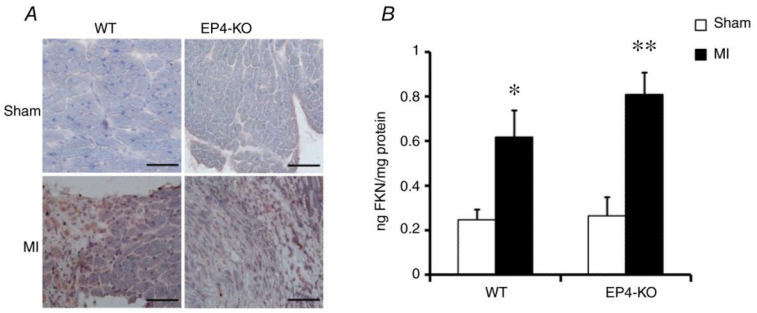

Figure 1. Effect of myocardial infarction (MI) on fractalkine (FKN) expression in the heart

A, representative immunohistochemistry staining of FKN. Scale bar is 100 μm. *B*, quantitative analysis of FKN in left ventricle samples by enzyme-linked immunosorbent assay. Data are presented as nanograms of FKN per milligram of protein. $n = 3$ per group. ***$P \leq 0.005$ *versus* respective sham-operated control mice. Abbreviations: EP4-KO, cardiac myocyte-selective deficiency of prostaglandin E_2 EP4 receptor subtype; and WT, wild-type.

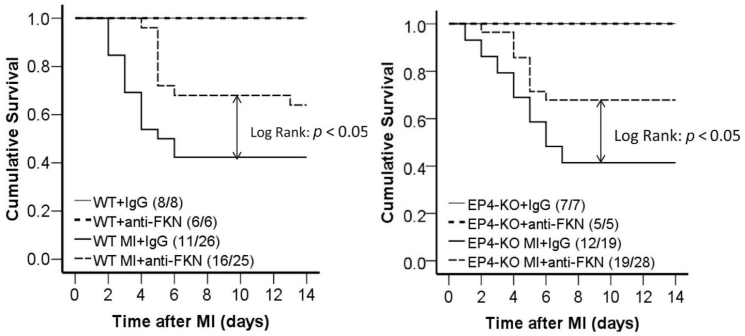

Figure 2. Kaplan–Meier curves demonstrating increased survival after MI in both wild-type (WT; left panel) and prostaglandin E_2 EP4 receptor subtype-deficient (EP4-KO) mice (right panel) treated with anti-FKN compared with IgG-treated control mice

Differences in survival between MI mice treated with anti-FKN *versus* IgG-treated control MI mice were tested with the log-rank test. $P < 0.05$ for both strains. The number of mice in each group is given as (number surviving/total number of mice) after the group description.

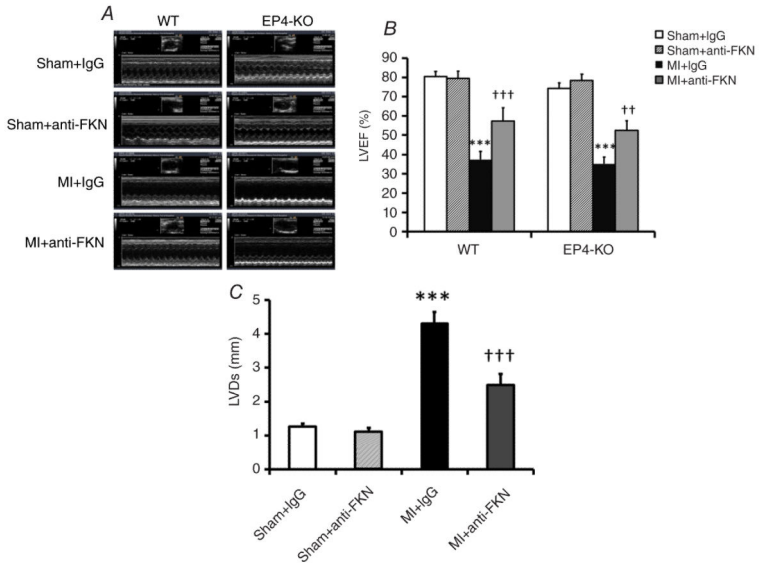

Figure 3. Effect of anti-FKN treatment on left ventricle ejection fraction (LVEF) and systolic dimension (LVDs) in WT and EP4-KO mice 2 weeks post-MI

A, representative M-mode echocardiograms. *B*, quantitative analysis of LVEF in WT and EP4-KO mice. *C*, quantitative analysis of LVDs in WT mice. n = 5–9 per group. ***P < 0.005 *versus* IgG-treated sham-operated mice; $^{\dagger\dagger}P$ < 0.01 and $^{\dagger\dagger\dagger}P$ < 0.005 *versus* IgG-treated MI mice.

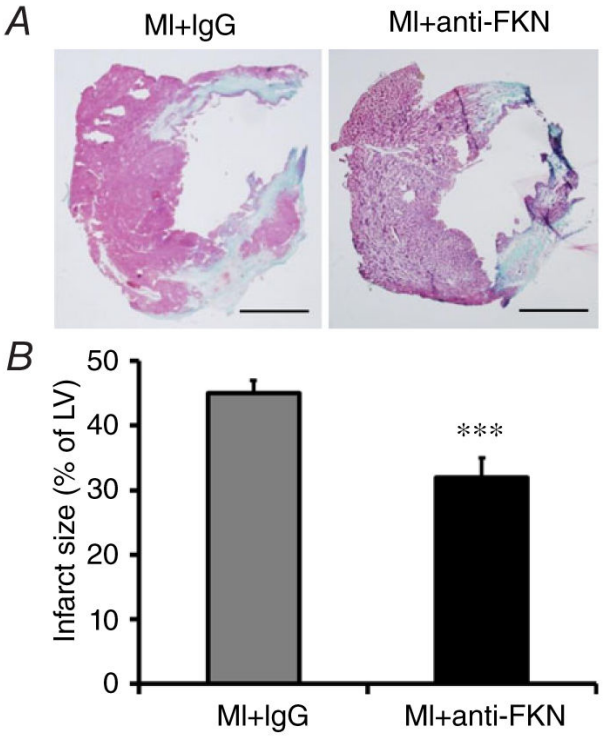

Figure 4. Effect of anti-FKN treatment on infarct size in WT mice 2 weeks post-MI

A, representative trichrome staining, showing infarcted portion of the LV. Scale bar is 500 μm. *B*, quantitative analysis of infarct size. n = 6–9 per group. ***$P < 0.005$ *versus* MI group treated with IgG.

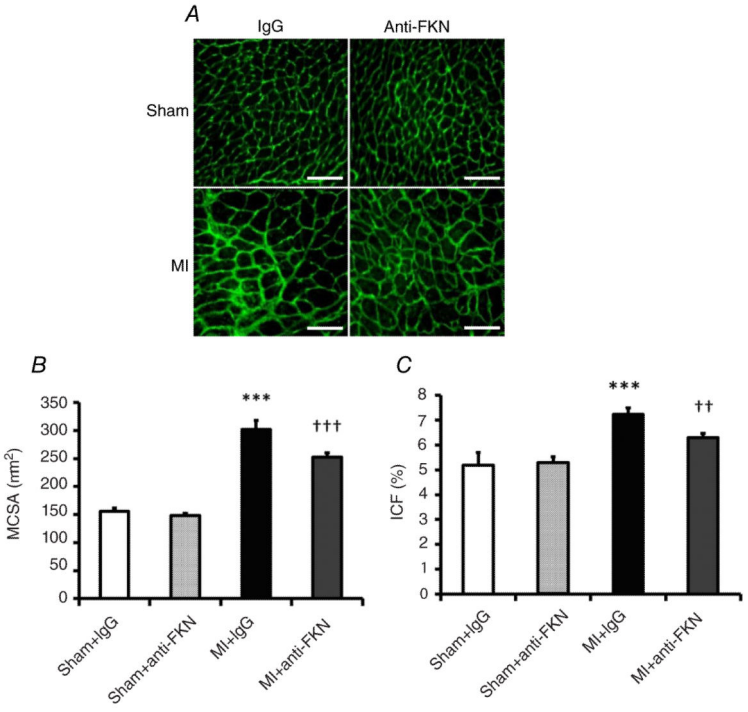

Figure 5. Effect of anti-FKN treatment on myocyte cross-sectional area (MCSA) and interstitial collagen fraction (ICF) in WT mice 2 weeks post-MI

A, representative images of myocyte size and interstitial collage deposition. Scale bar is 100 μm. Quantitative analysis of MCSA (*B*) and ICF (*C*). n = 5–9 per group. ***$P < 0.005$ *versus* IgG-treated sham-operated mice; $^{\dagger\dagger}P < 0.01$ and $^{\dagger\dagger\dagger}P < 0.005$ *versus* MI group treated with IgG.

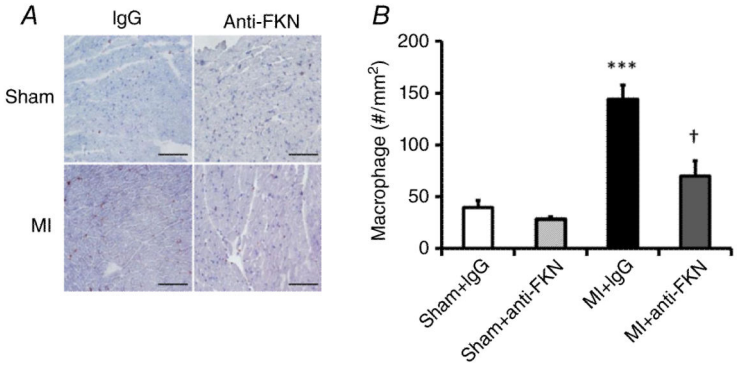

Figure 6. Effect of anti-FKN treatment on macrophage infiltration in WT mice 2 weeks post-MI

A, representative immunohistochemical staining showing infiltrated macrophages ($CD68^+$ cells, purple colour) in the left ventricle. Scale bar is 100 μm. *B*, quantitative analysis of macrophage infiltration. n = 4–9 per group. ***$P < 0.005$ *versus* IgG-treated sham-operated mice; $^{\dagger}P < 0.05$ *versus* MI group treated with IgG.

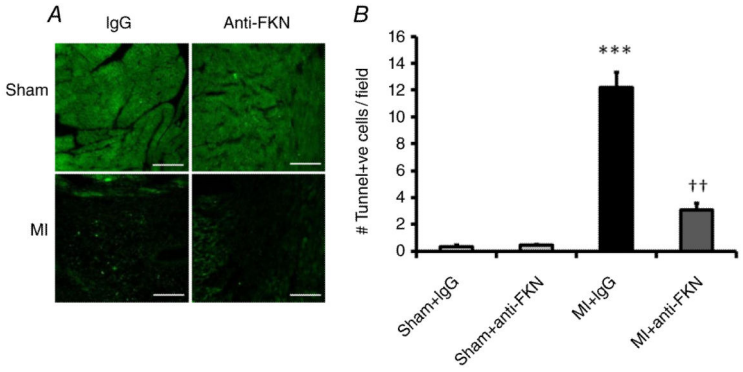

Figure 7. Effect of anti-FKN treatment on apoptosis in WT mice 2 weeks post-MI

A, representative images of TUNEL staining for apoptosis (bright green spots) in the left ventricle. Scale bar is 200 μm. *B*, quantitative analysis of apoptotic index. $n = 3$ per group. ***$P < 0.005$ *versus* IgG-treated sham-operated mice; $^{\dagger\dagger}P < 0.01$ *versus* MI group treated with IgG.

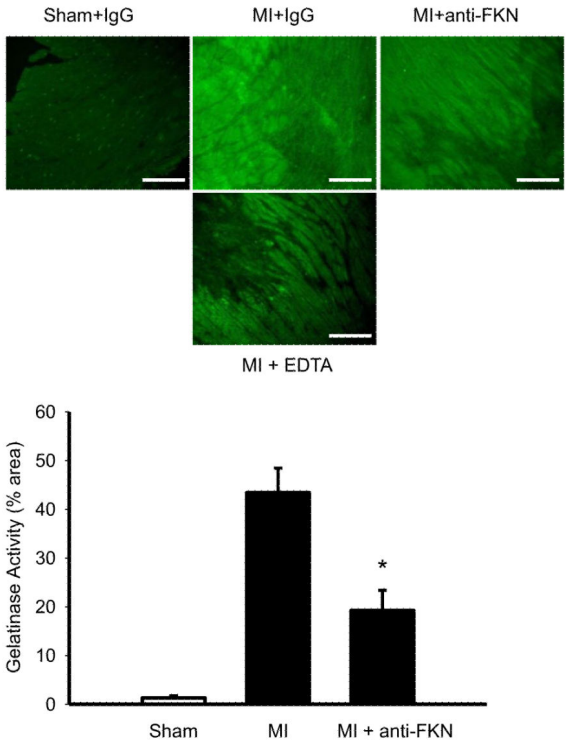

Figure 8. ***In situ*** **zymography, showing gelatinase activity (green fluorescence) in the left ventricle**

The MI + EDTA slide is a control indicating suppression of the fluorescence (inhibiting gelatinase activity) with EDTA. Scale bar is 200 μm. Images are representative of three different animals. Bar graph shows quantification of gelatinase activity expressed as the percentage area after threshold with n = 3 mice.

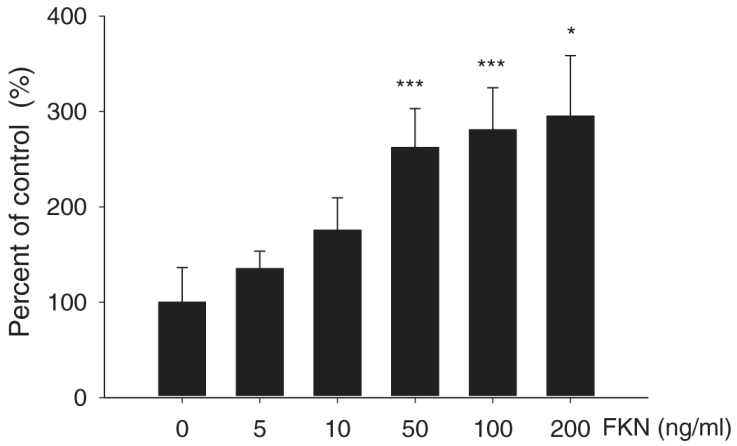

Figure 9. Effect of FKN on adult cardiac fibroblast proliferation

Adult cardiac fibroblasts at passage 3 were treated with the stated concentrations of FKN for 24 h in serum-free media, and proliferation was assessed by the MTT assay with absorbance measured at 550 nm. Histogram shows FKN concentration in nanograms per millilitre on the *x*-axis, and the *y*-axis is percentage of control, with the absorbance values in vehicle-treated cells set at 100%. $n = 5$ separate fibroblast preparations. *$P < 0.05$ and ***$P < 0.005$ compared with vehicle control.

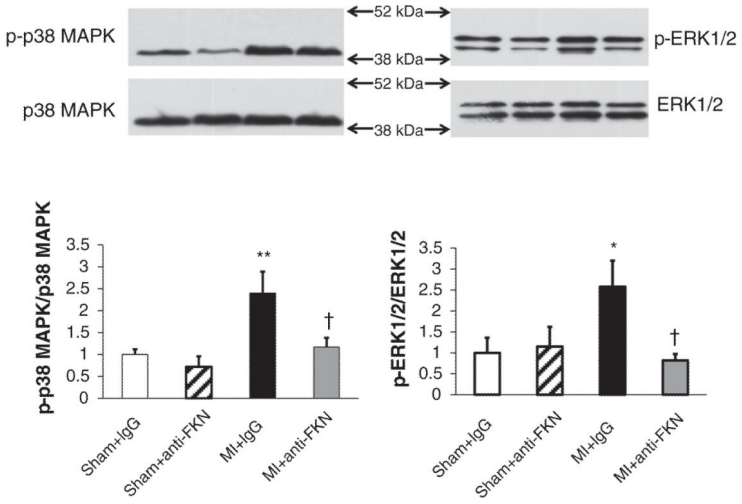

Figure 10. Samples of left ventricle were examined for p38 mitogen-activated protein kinase (MAPK; left panels) and extracellular signal-related kinase 1/2 (ERK1/2; right panels) by Western blotting

Representative Western blots for WT mice are shown in the upper part of the figure and quantitative data are shown in the bar graphs below. Phosphorylated p38 and ERK1/2 and are corrected to total p38 and ERK1/2, respectively. **P* < 0.05 and ***P* < 0.01 *versus* IgG-treated sham-operated mice; †*P* < 0.05 *versus* MI mice treated with IgG. *n* = 3 for each group.

Table 1

Echocardiography data of wild-type mice treated with anti-fractalkine

Parameter	Sham + IgG (*n* = 8)	Sham + anti-FKN (*n* = 6)	MI + IgG (*n* = 7)	MI + anti-FKN (*n* = 7)
HR (beats min^{-1})	691 ± 21	712 ± 14	708 ± 8	675 ± 29
BW (g)	30.9 ± 1.7	27.8 ± 0.8	29.7 ± 0.7	31.3 ± 0.8
LVEF (%)	80.40 ± 2.8	79.40 ± 3.9	37.44 ± 4.3**	57.23 ± 6.9††
LVDd (mm)	2.75 ± 0.09	2.80 ± 0.12	5.03 ± 0.31**	3.74 ± 0.35††
LVDs (mm)	1.26 ± 0.09	1.10 ± 0.11	4.30 ± 0.44***	2.48 ± 0.44†
PWTd (mm)	0.99 ± 0.08	0.90 ± 0.04	0.76 ± 0.04*	0.95 ± 0.07
LVAs (mm^2)	0.90 ± 0.16	0.90 ± 0.22	9.68 ± 1.97**	4.27 ± 1.18†
LVAd (mm^2)	4.64 ± 0.59	4.1 ± 0.25	14.66 ± 2.44**	8.75 ± 1.51
SF (%)	54.17 ± 2.70	59.1 ± 4.18	19.04 ± 4.74***	33.66 ± 6.29

Abbreviations: BW, body weight; FKN, fractalkine; HR, heart rate; LVAd, left ventricular area at diastole; LVAs, left ventricular area at systole; LVDd, left ventricular dimension at diastole; LVDs, left ventricular dimension at systole; LVEF, left ventricular ejection fraction; MI, myocardial infarction; PWTd, posterior wall thickness at diastole; and SF, shortening fraction.

* $P < 0.05$,

** $P < 0.01$ and

*** $P < 0.005$ *versus* sham MI;

† $P < 0.05$ and

†† $P < 0.01$ *versus* MI + IgG.